Characterization of the Branched-Photocycle Intermediates P and Q of Bacteriorhodopsin

Nathan B. Gillespie,[#] Kevin J. Wise,[#] Lei Ren,[#] Jeffrey A. Stuart,[†] Duane L. Marcy,[†] Jason Hillebrecht,[#] Qun Li,[†] Lavoisier Ramos,[#] Kevin Jordan,[#] Sean Fyvie,[#] and Robert R. Birge*[,#,†]

Departments of Chemistry and of Molecular and Cell Biology, University of Connecticut, 55 North Eagleville Road, Storrs, Connecticut 06269, and W. M. Keck Center for Molecular Electronics and Department of Chemistry, Syracuse University, 111 College Place, Syracuse, New York 13244-4100

Received: May 16, 2002; In Final Form: September 25, 2002

The bacteriorhodopsin branched-photocycle intermediates **P** and **Q** are studied with respect to chromophore isomeric content, photochemical origin, kinetic heterogeneity, and photoreversibility. These blue-shifted species are compared to products with similar spectroscopic properties generated via thermal denaturation. We observe that the thermal and photochemical species differ in both isomeric content and binding site environment. Sequential two-photon activation of glycerol suspensions of bacteriorhodopsin containing low concentrations of water (<15% v/v water/glycerol) form high yields of **P** state but almost no **Q** state. This observation is attributed to the role that water plays in the hydrolysis reaction that converts the **P** state to **Q**. Relatively large photostationary state populations of both intermediates can be generated in both 85% v/v glycerol suspensions and polyacrylamide gels. At ambient temperature, both intermediates can be fully converted back to **bR** with blue light. Chromophore extraction and HPLC analysis reveal that **P**, **Q**, and the spectrally similar thermal products have a 9-cis retinal chromophore. The thermal products are also found to contain small amounts of the 7-cis isomer. Time-resolved spectroscopy reveals that the **P** state is actually comprised of two components with maximum absorptivities at 445 and 525 nm. The molar absorptivities of the chromophore band maxima of the **P** and **Q** states in an 85% v/v glycerol/water suspension at pH 7 are $\epsilon(\mathbf{P}_{445}) = 47\,000$, $\epsilon(\mathbf{P}_{525}) = 39\,000$, and $\epsilon(\mathbf{Q}) = 33\,000\ M^{-1}\ cm^{-1}$. Kinetic analyses support previous studies indicating that the **P** state is formed predominantly from the **O** state, which is consistent with the branched-photocycle model. However, other paths to the **P** state are possible, including direct excitation of the small population of blue membrane present in solution. We examine the hypothesis that the branched-photocycle evolved as a photochromic sunscreen for UVA and UVB protection.

1. Introduction

Bacteriorhodopsin (BR) is the light-transducing protein embedded in the purple membrane of the archaeon *Halobacterium salinarum* (aka *Halobacterium halobium* or *Halobacterium salinarium*). Archae are informally called *archaebacteria*, but they are not bacteria with respect to formal classification. On the basis of physiology, the archae are organized into three types: methanogens (prokaryotes that produce methane); extreme halophiles (prokaryotes that live at very high concentrations of salt); and extreme (hyper) thermophiles (prokaryotes that live at high temperatures). *H. salinarum* is an extreme halophile that lives in natural environments such as the Dead Sea, the Great Salt Lake, or salt flats where the salt concentration is above that found in the oceans (as high as 5 M or 25% NaCl by weight). *H. salinarum* requires salt for growth and for cell wall, ribosome, and enzyme stability. The organism adapts to low oxygen availability by synthesizing the purple membrane, which it uses for photosynthetic energy production. The predominant protein in the purple membrane, BR, converts light into a proton gradient, which is subsequently used to synthesize ATP. This process is the only example in nature of nonphotosynthetic photophosphorylation. But *H. salinarum* is also a heterotroph that preferentially respires by aerobic means; the organism does not rely on the purple membrane for energy when the concentration of oxygen is sufficient to sustain respiration. This capability is important from a bioengineering standpoint, because it allows genetic manipulation of the protein to produce useful materials that are inefficient or inactive proton pumps. This observation may also provide a perspective on the potential biological relevance of the branched photocycle.

The proton-pumping process of BR is initiated when the protein-bound chromophore, the protonated Schiff base of all-trans retinal, absorbs a photon of light and undergoes the photocycle schematically shown in Figure 1.[1] Although many aspects of the proton pumping mechanism remain to be discovered, much has been learned about the molecular details during the past few years.[2] The primary photochemical event involves an all-trans to 13-cis photoisomerization that produces the first thermally trappable intermediate labeled **K**. The proton pumping mechanism is facilitated through a series of dark reactions which form, in succession, the **L**, **M**, **N** and **O**, intermediates (see Figure 1b). The isomerization of the chromophore creates an electrostatic environment that destabilizes the protonated Schiff base, resulting in deprotonation of the chromophore and protonation of the nearby Asp-85 residue. This process generates the **M** state, which is blue-shifted because the chromophore is now unprotonated. Subsequent dark reac-

* To whom correspondence should be addressed. Phone: 860-486-6720. Fax: 860-486-2981. E-mail: rbirge@uconn.edu.
[#] University of Connecticut.
[†] Syracuse University.

10.1021/jp021221p CCC: $22.00
Published on Web 11/21/2002

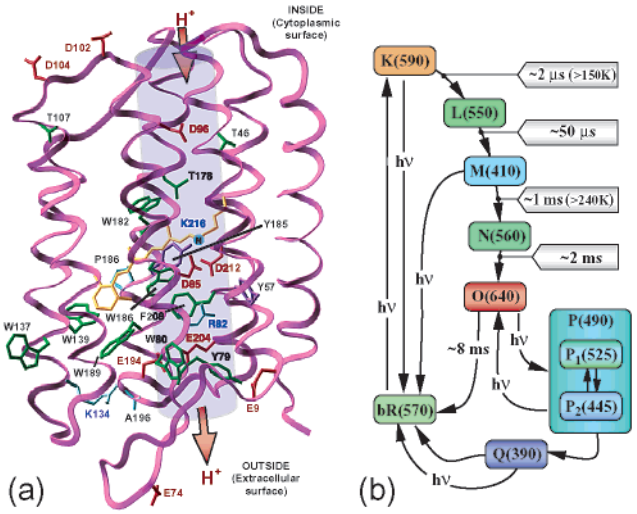

Figure 1. A schematic representation of (a) the bacteriorhodopsin tertiary structure and (b) the main photocycle and the branching reactions studied here. The structure is based on the crystal coordinates,[1] the proton pumping channel is shown in blue, and selected residues are indicated for reference. The chromophore is shown in yellow.

tions transfer the proton from Asp-85 down to the Glu-194 and Glu-204 region, and the chromophore is reprotonated through donation of a proton from Asp-96. The branching reaction that is the subject of this study is also shown in Figure 1b. The branch involves photoactivation of the **O** state by red light, which induces all-trans → 9-cis photochemistry.[3] However, the 9-cis chromophore is not stable in the binding site, and hydrolysis of the Schiff base takes place to produce 9-cis retinal.[3] The latter unbound chromophore is constrained to the binding site region, because the kinked 9-cis species can neither enter nor exit the binding site. The result is formation of the **Q** state ($\lambda_{max} \approx 390$ nm), a stable species with a barrier of ~190 kJ mol^{-1} to thermal reformation of the **bR** state.[4]

As the functional element of two-dimensional memory applications, BR can operate at the diffraction limit while providing high cyclicity, efficiency, and sensitivity. Light-adapted BR (**bR**) and the blue-shifted **M** state provide a bistable set with excellent spectral and refractive properties for real-time holography.[5,6] The use of the **M** state as a binary component in long-term holographic storage is currently hindered by the lack of a chemically or mutagenically modified protein with a long-lived **M** state at ambient temperature. One option is to use blue-membrane-like or D85N-based variants,[7−9] but no solution to the poor cyclicity of these systems has yet been found. An attractive alternative is provided by the long-lived **Q** state, which has a lifetime of 7−12 years at ambient temperature. This state has an absorption maximum that is blue-shifted relative to the **M** state and hence provides enhanced refractive and diffractive properties in addition to an extended lifetime. More recently, the fact that the **Q** state is generated via a sequential two-photon process has allowed the development of paged three-dimensional memories.[4] Despite their potential importance in bioelectronics devices, relatively little is known about the properties of the **P** and **Q** states. The present investigation was initiated to provide a better understanding of the photochemical origin and stability of these states and to probe the effect of solvent environment on their properties.

Popp et al. were first to report formation of the **P** and **Q** states.[3] These investigators carried out sophisticated holographic studies to demonstrate that these states originated via photochemical activation of the **O** state. The **P** and **Q** states were shown to contain 9-cis retinal chromophores and to revert photochemically back to **bR** with blue light.[3] The studies reported here confirm the principal conclusions of Popp et al. but in addition conclude that the **P** state is actually a mixture of two species in dynamic equilibrium. Dancsházy and co-workers have used both photochemistry and thermal stress to reinvestigate the long-lived, blue-shifted states of bacteriorhodopsin.[10,11] They conclude that formation of the photochemical and thermal states results in partial denaturation of the protein. Experiments in this paper demonstrate that under the appropriate conditions, the blue-shifted states can be fully reverted back to **bR** without imposing any permanent change in the protein. This conclusion is of significant importance to any proposed use of this protein in holographic or three-dimensional optical memories.

Although the principal impetus for initiating these studies was the importance of these blue-shifted states to the development of BR-based photonic devices, a better understanding of the origin and properties of these states has fundamental importance. Nature has optimized the binding sites of the retinal-based light-transducing proteins to provide highly efficient bond-specific photochemistry. The rhodopsins and the cone pigments of the vertebrate and invertebrate photoreceptors have been optimized through evolution to select for and enhance the efficiency of the 11-cis to 11-trans photochemical process.[12,13] Bacteriorhodopsin has been optimized through evolution to enhance the efficiency of the all-trans to 13-cis photochemical process.[14,15] It remains to be explained why the independent evolutionary enhancement of these systems has converged on primary event quantum efficiencies that are experimentally identical ($\Phi_{PE} \cong 0.65$). Does this value of Φ_{PE} represent some limiting value for bond-specific retinal photochemistry, or is this a simple coincidence? Answers to such questions require a more detailed experimental understanding of how the photochemistry of the retinal chromophores is directed by protein−chromophore interactions. Through studies of side reactions, such as the direct and indirect formation of the **P** and **Q** states in bacteriorhodopsin, new insights into the underlying mechanisms of protein-mediated photochemistry are possible.

2. Materials and Methods

Bacteriorhodopsin membrane fractions were purified according to standard procedures.[16,17] In experiments designed to explore the effect of water content in purple membrane (PM), suspensions were prepared with low water content in glycerol (85%, 90%, and >95% glycerol or 15%, 10%, and <5% water by volume) in polymethacrylate semimicrocuvettes (Fisher no. 14-385-938). PM pellets produced via low-pressure centrifugation (Eppendorf vacufuge, 240×**g** at <20 mbar vacuum, 30 °C) were mixed with the appropriate glycerol/water solution, followed by sonication at 20 kHz (Heat Systems cell disrupter model W-225 R) to disperse aggregates. Mixtures were then irradiated at 647 nm (1.8 W/cm^2, 6 mm diameter beam) from a Coherent Innova 300 krypton ion gas laser for a total of 45 min. The samples were subsequently homogenized prior to analysis by UV−visible spectroscopy (Cary 50 UV−vis spectrometer).

Steady-state and time-resolved kinetic experiments were performed on 85% v/v glycerol to water purple membrane suspensions (1.2 OD per 1 mm path, pH 7, 50 mM phosphate buffer, 22 ± 1 °C) in a 1 mm path length quartz flow cuvette (Starna Cells, 73.1F) sealed with Parafilm. Steady-state spectra were taken on a Cary 50 UV−visible spectrometer (Varian, Inc.)

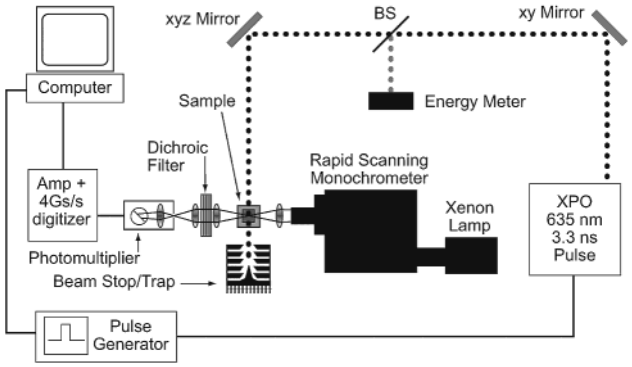

Figure 2. Schematic of the apparatus used in the sustained illumination and temporal kinetic studies.

following exposure to red light from a 50 W mercury−xenon arc lamp passed through a 647 ± 40 nm band-pass filter (30 ± 3 mW/cm^2) (Melles Griot no. 03FIV048). Light adaptation and partial regeneration were accomplished via exposure to 550 ± 20 nm (10 ± 2 mW/cm^2) (Melles Griot no. 03FIV044) light from the same lamp. Full regeneration was attained with a 400 ± 20 nm (10 ± 2 mW/cm^2) (Melles Griot no. 03FIV026) band-pass filter. The average intensity from the lamp was measured by a wavelength- and intensity-calibrated power meter (Coherent LM-2 interfaced with a Coherent Labmaster Ultima data acquisition unit). Analogous experiments were performed on purple membrane fractions immobilized in a 10% cross-linked polyacrylamide matrix buffered in 50 mM phosphate at pH 8 in 1 cm methacrylate cuvettes. Immobilized purple membrane suspensions were exposed to ∼100 mW/cm^2 from a 50 W mercury−xenon arc lamp with a glass cutoff filter (λ > 620 nm) at 40 °C, followed by exposure to a long-wave UV lamp centered at 365 nm (UVP, Inc. UVL-14). Spectra were taken of the resulting ∼1 cm^2 photoconverted volume (i.e., yellow photoproduct) with a diode array UV−visible spectrometer (HP 8453).

In the time-resolved experiments, samples at 40 °C were exposed to 635 nm, 3.3 ns pulse-width emission from an optical parametric oscillator (OPO) pumped by the third harmonic of a Nd:YAG system (Coherent Infinity-XPO). The energy of each pulse was measured by a calibrated energy meter (Ophir PE50-BB interfaced to an Ophir Laserstar acquisition unit). A rapid scanning monochromator (RSM) system (OLIS instruments, Inc. RSM-1000 stopped flow) observed the sample spectrum (360−590 nm, 1000 scans were collected and averaged each second) orthogonal to the incident beam, while a constant-temperature bath maintained the temperature of the samples within 1 °C (Julabo F30-C, modified by OLIS instruments, Inc.). To screen out the intense 635 nm emission from the OPO, a dichroic filter (CVI Laser, Inc. CP-SC-590-1.00) was placed in front of the sample photomultiplier in the RSM system. A schematic of the time-resolved apparatus is illustrated in Figure 2. A reference spectrum was taken at the start of each experiment, and the subsequent difference spectrum was monitored by using the RSM system.

The chromophore analysis studies were performed in a dim red light environment using the method of P. Scherrer et al.[18] Using a vortex mixer, we agitated 100 μL of each sample for 1 min with 250 μL of ice-cold ethanol in a centrifuge tube. A total of 500 μl of hexane was then added, and samples were agitated for 2 min and subsequently centrifuged for 1 min. The resulting organic layer was transferred to a sample vial with a Pasteur pipet and immediately analyzed by HPLC (Waters 600E multisolvent delivery system with a Water 2487 dual wavelength detector) in a method adapted from recent work by G. Noll and C. Becker.[19] Two Prep Nova-Pak HR Silica columns (3.9 × 300 mm^2, Waters, Milford, MA) in series provided the stationary phase. The mobile phase, flowing at 1.5 mL/min, was composed of 93% hexane and 7% *tert*-methyl butyl ether (TBME).

Thermal denaturation studies were carried out on 85% v/v glycerol suspensions of purple membrane in a 100 μL quartz cuvette (Starna cells 16.100F-Q-10). An electronically controlled, water-cooled, Peltier-driven sample holder (Varian no. 00 10074 00) maintained the temperature, while the spectra were sampled with a Cary 50 UV−visible spectrometer. Samples were equilibrated for 10 min at the specified temperature prior to collecting the spectra.

3. Results and Discussion

The experiments and observations discussed below provide evidence that the **P** state is actually comprised of two components with maximum absorptivities at 445 and 525 nm. However, under most experimental conditions, only a single species is observed with an absorption maximum at 440−450 nm (mostly $\mathbf{P}_{445}$ with small amounts of **Q** likely present) or 490 nm (roughly equal mixtures of $\mathbf{P}_{445}$ and $\mathbf{P}_{525}$). To be consistent with the literature, such mixtures are referred to as the **P** state when differentiation into the $\mathbf{P}_{445}$ and $\mathbf{P}_{525}$ components either is not possible or was not attempted. The extraction experiments carried out in this study indicate that both $\mathbf{P}_{445}$ and $\mathbf{P}_{525}$ have 9-cis retinal chromophores. The absorption spectra and previous studies of the blue membrane provide strong evidence that both $\mathbf{P}_{445}$ and $\mathbf{P}_{525}$ have protonated Schiff base chromophores.[3,9,20−23] We will speculate on the molecular differences of these two species below.

Additional evidence is provided in support of the model proposed by Popp et al.[3] that the **Q** state is comprised of 9-cis retinal constrained somewhere inside the chromophore binding site. It is thus likely that there are many forms of the **Q** state characterized by different locations and orientations of the free chromophore inside the binding site. Upon excitation with blue light, the 9-cis retinal chromophore isomerizes to all-trans and recombines rapidly with lysine-216 to form **bR**. This process involves at least one intermediate, labeled Θ, characterized by all-trans retinal not covalently bound to the protein. Studies are underway to characterize the nature of this short-lived Θ species, which is normally not shown in diagrams (e.g., Figure 1).

a. Hydration Experiments in Glycerol. A sample of bacteriorhodopsin suspended in 85% (v/v) glycerol was illuminated at 647 nm for 45 min, and the results are shown in Figure 3a,b. Illumination generates an initial rise at 445 nm due to formation of the **P** state, which is evident upon subtraction of the light-adapted **bR** spectrum. After the sample was left in the dark for 15 h, a 390 nm absorbing species formed that was assigned as the **Q** state. These observations provide evidence that the **P** state is a precursor to the **Q** state and that **P** can thermally transform to **Q** upon formation via excitation of the **O** state. Note that no significant regeneration of **bR** (560−570 nm) from **P** can be seen following 15 h in the dark, an indication that the **bR** resting state does not thermally regenerate from **P** under the conditions of this study.

The **Q** state is thermally produced from **P** as a result of hydrolysis of the Schiff-base linkage binding the retinal chromophore to the protein. Therefore, if all water were removed from the sample, no transition from **P** to **Q** would be expected. A sample of bacteriorhodopsin was suspended in >95% glycerol and tested under conditions identical to those described above (Figure 3c,d). There was no blue-shift of the sample over time.

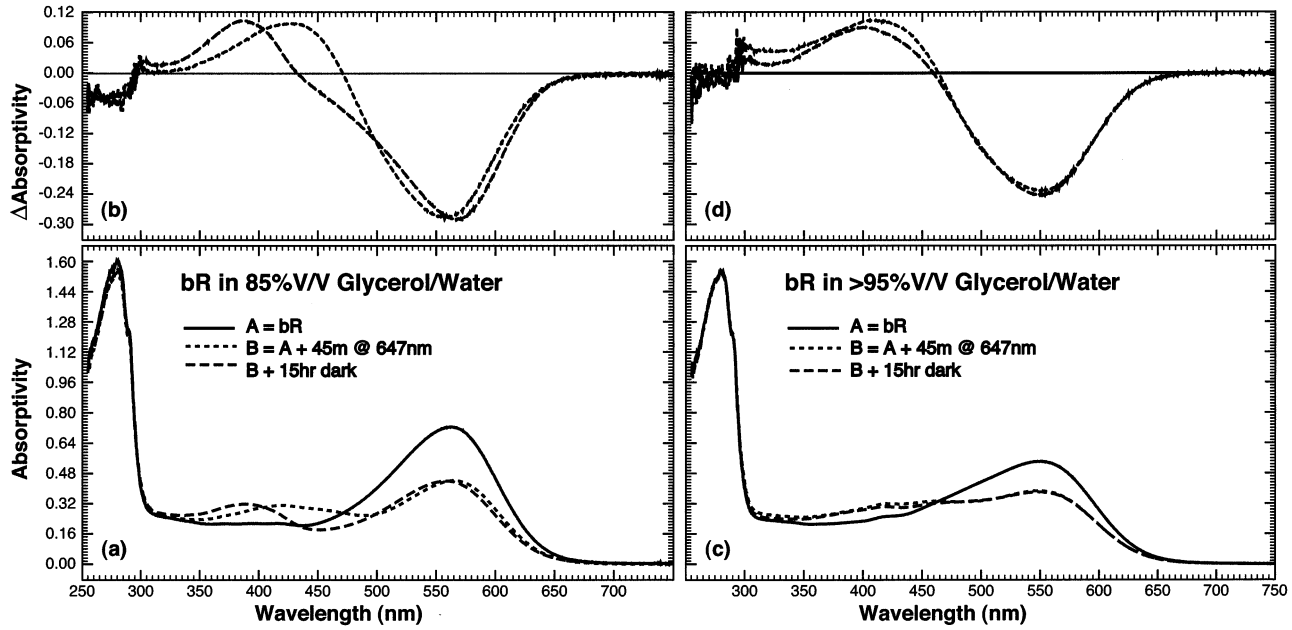

Figure 3. Absolute (a,c) and difference (b,d) spectra of the **P** and **Q** states in samples containing 85% v/v (left) and >95% v/v (right) glycerol following 647 nm irradiation at 1.8 W/cm^2 (short dashes) followed by 15 h in the dark (long dashes).

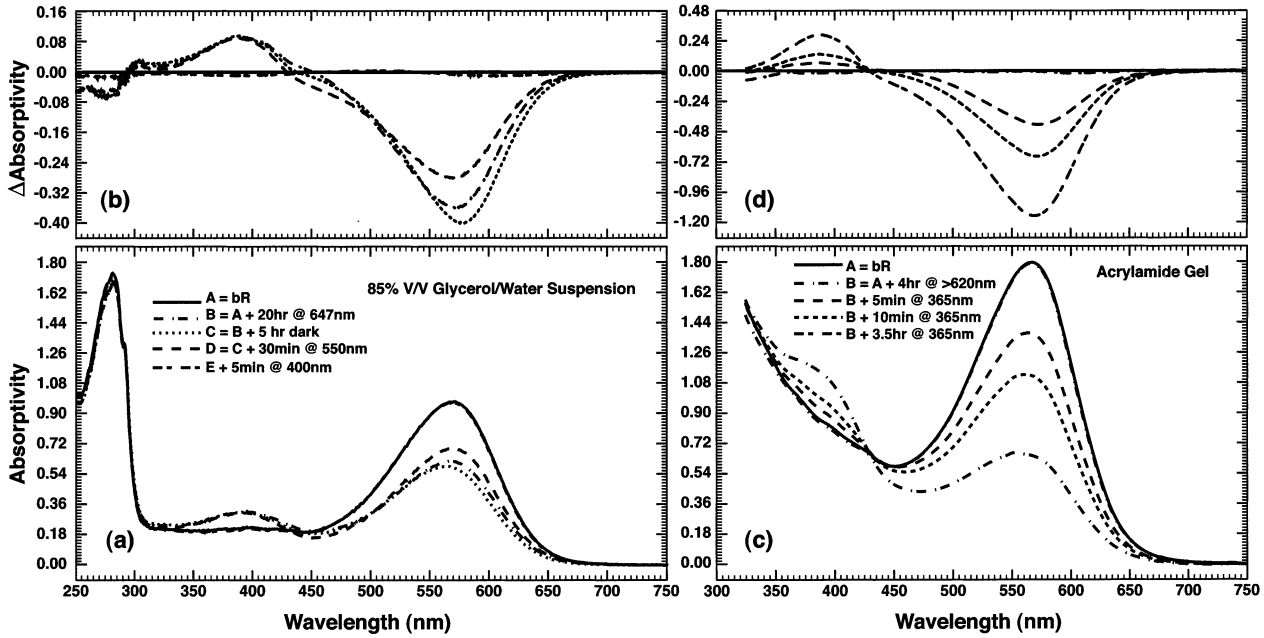

Figure 4. Regeneration of light-adapted bacteriorhodopsin (**bR**) at 40 °C from the **P** and **Q** states in 85% v/v glycerol/water at pH 7 (left) and in a hydrated acrylamide gel at pH 8 (right). The glycerol-containing sample was left in the dark for 5 h and then the spectrum was taken to demonstrate that a thermal equilibrium exists between **P** and **Q**. The difference spectra are on top (b,d) and the absolute spectra are on the bottom (a,c).

Furthermore, no significant changes were observed after 15 h in the dark, consistent with the interpretation that water must be present in the binding site for the hydrolysis reaction to proceed. This indicates either that BR is trapped in the **P** state or that the **P** → **Q** transition is severely inhibited.

b. Regeneration of the P and Q States. **P** and **Q** state generation/regeneration experiments were performed on bacteriorhodopsin in both 85% (v/v) glycerol suspensions and polyacrylamide gels. The results of these experiments are shown in Figure 4. In Figure 4a, an 85% glycerol/water suspension of BR was successively illuminated with red, green, and violet light at ambient conditions (22 ± 1 °C). Illumination with green light (550 ± 20 nm) resulted in full regeneration of **bR** from the **P** state but no significant regeneration from the **Q** state (Figure 4a), indicating that **Q** does not absorb substantially in this spectral region. However, violet light (400 ± 20 nm) regenerated **bR** from both **P** and **Q**. Full recovery of the protein is evident from the complete regeneration of not only the 568 nm peak in this spectrum but the 280 nm peak as well. A polyacrylamide-suspended sample was illuminated for 4 h with a cutoff filter (>620 nm) at 40 °C to obtain the first spectrum shown in Figure 4c. The unshifting isosbestic point at 430 nm in this spectrum is a clear indication that **bR** and **Q** are the dominant species in this sample, while **P** persists in much smaller quantities in the polyacrylamide matrix. This observation is consistent with the observation that high water content

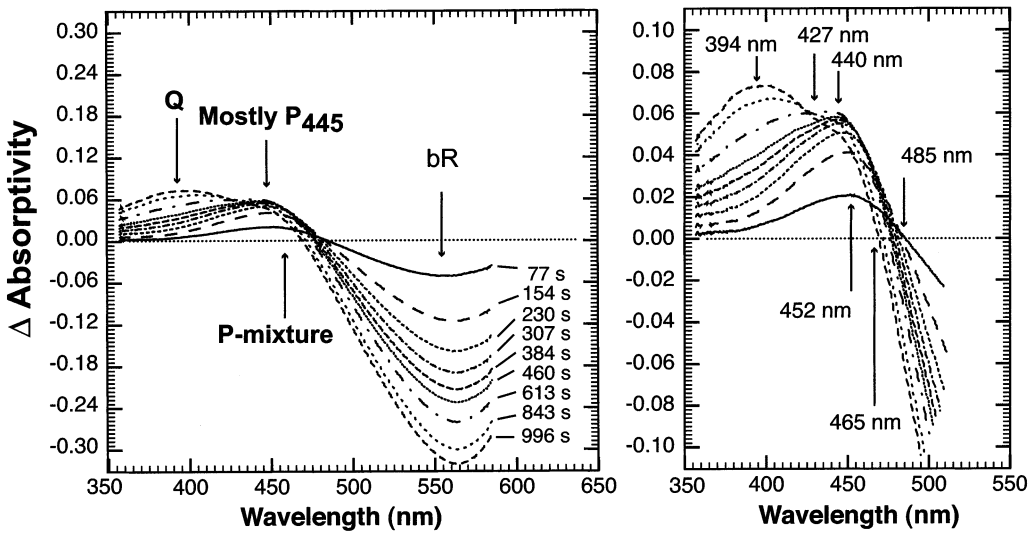

Figure 5. Time-resolved difference spectra of a purple membrane 85% v/v glycerol suspension during illumination at 635 nm and 50 Hz. The average energy density was 40 mJ/cm^2, and the average intensity was 2 W/cm^2. The maximum positive difference blue-shifts from 452 to 440 nm and ultimately to 394 nm.

enhances Schiff base hydrolysis. Approximately 50% regeneration occurs after only 5 min illumination with UV light centered at 365 nm. Illumination with UV light for 3.5 h results in 100% regeneration of the chromophore peak from the 390 nm absorbing species. The difference spectra in Figure 4b,d show that the **Q** state ($\lambda_{max} \approx 380$ nm) can be fully converted back to **bR** via UV irradiation in both sample preparations. This observation is in contrast to the recent work by Dancsházy and Tokaji that shows only partial regeneration after 30 min of illumination with blue light.[11] Although the latter studies were carried out on samples at 60 °C, the authors state that there is little difference between the data collected at 60 and 20 °C. We find that samples below 45 °C regenerate with high cyclicity.

The elevated temperature (40 vs ~22 °C) and higher intensity (100 vs 30 mW/cm^2) required to achieve similar conversion of **bR** to **Q** in an aqueous gel are an indication that the net quantum yield of **P** formation is lower and more temperature sensitive in a polyacrylamide gel than that in a hydration-limited glycerol suspension. At room temperature (22 ± 1 °C), negligible conversion of **bR** to **Q** is found after exposing BR to illumination at 620 nm in polyacrylamide with the same intensity (100 mW/cm^2) and time span (5 h).

The **P** and **Q** state spectra in Figure 4a, generated after 20 h of exposure at 647 nm, can be interpreted as the result of an equilibrium condition. This interpretation is supported by the lack of a substantial blue shift in the spectrum after 5 h in the dark and by the fact that the 380 nm peak in the difference spectrum is unchanged following partial regeneration of the **bR** state upon exposure to 550 nm light for 30 min. Because **Q** formation requires water, much more of the **P** state is present in equilibrium with **Q** in low water content environments.

c. Sustained Illumination Experiments and Calculated Spectra. Figure 5 presents a set of time-resolved difference spectra obtained at 40 °C with steady-state pulsed illumination at a repetition rate of 50 Hz at 635 nm. The sample was equilibrated at 40 °C for at least 15 min to minimize any thermal changes in the spectrum. The sample was then illuminated for 30 s to ensure that the fast photointermediates (**M**, **O**, etc.) had reached photostationary state; thus, the reference spectrum in these difference spectra is the photostationary state of **bR** and its fast photointermediates. The first isosbestic point in these spectra shifts from 485 to 465 nm, indicating that the **P** state is a two-species mixture. The initial spectrum (maximum difference at 460 nm) has virtually the same isosbestic point (485 nm) that Popp et al. observed for **P** state in thin films (483 nm).[3] Under these conditions, however, the maximum quickly blue-shifts to 440 nm followed by a slower shift to 394 nm. A second isosbestic point forms at 427 nm after ~600 s, indicating that the red-absorbing form of the **P** state found in the earlier spectra has all but disappeared. The faster kinetics of the **P** → **Q** transition in this experiment (~10 min vs 5 h in Figure 4) can be attributed to an increase in temperature (40 vs 22 °C in Figure 4).

The spectra in Figure 6 were calculated from steady-state spectroscopic investigations of **P** and **Q** in an 85% glycerol suspension at pH 7. The spectra were calculated via singular value decomposition of several sets of steady-state regeneration spectra like those shown in Figure 4a. The results were smoothed using a 5 nm slit width, and we believe the fine structure observed in the 280 nm band of the $\mathbf{P}_{525}$ state to be an artifact of the decomposition process owing to a low signal-to-noise ratio in the spectra of the **P** state in the 280 nm region. The band maxima and selected extinction coefficients are shown in Table 1. The **Q** state spectrum that we generated is in good agreement with those obtained in previous studies.[3,10,11]

The **P** state saturates to a photostationary state when exposed to red light at 647 ± 40 nm, indicating that this state has some absorbance in this region. As indicated in the time-resolved study above, the **P** state in this system is believed to be comprised of two components. Deconvolution of the spectra from two different regeneration experiments led to the results shown in Figure 6. The long-wavelength state, $\mathbf{P}_{525}$ (λ_{max}= 525 nm), is believed to be the primary branching photoproduct and appears to be quite unstable and inhomogeneous. We speculate that the inhomogeneity is associated with a variety of protein conformations unfavorable to the 9-cis photoproduct. This inhomogeneous set of protein−chromophore interactions will destabilize the ground state and generate a red-shifted absorption band relative to the second **P** state. The $\mathbf{P}_{525}$ state thermally rearranges quickly to form $\mathbf{P}_{445}$ (λ_{max}= 445 nm), which is considerably more homogeneous and stable when the water content in the glycerol solution is low (<15% water by volume). This two-state model can explain why the electronic spectrum of the predominant component reported here, $\mathbf{P}_{445}$, is blue-shifted

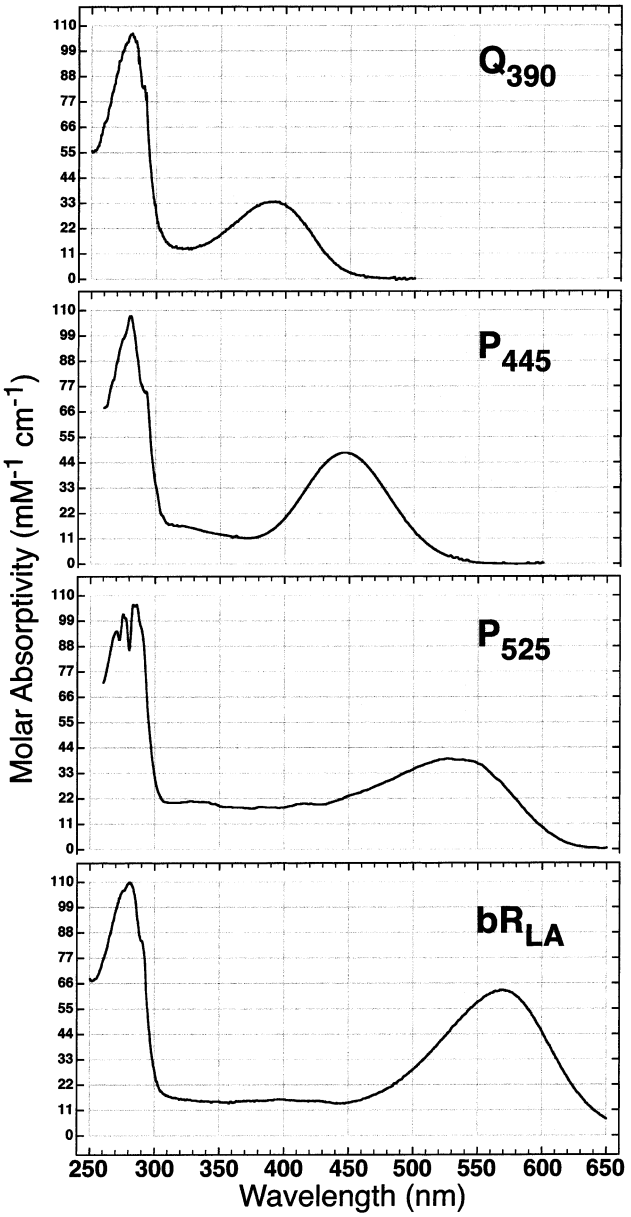

Figure 6. Calculated spectra of the two **P** states and the **Q** state as compared to **bR** (light-adapted BR). The molar absorptivities are based on a value of 63 000 M^{-1} cm^{-1} at 568 nm for **bR**.

TABLE 1: Summary of Calculated Molar Extinction Coefficients of P and Q State Species Based on an Extinction Coefficient of 63 000 M^{-1} cm^{-1} at 568 nm for bR

state[a]	ϵ at 280 nm (M^{-1} cm^{-1})	λ_{max} (nm)	ϵ (M^{-1} cm^{-1})
bR	110 000	568	63 000
$\mathbf{P}_{445}$ (or $\mathbf{P}_2$)	109 000	445	47 000
$\mathbf{P}_{525}$ (or $\mathbf{P}_1$)	108 000	525	39 000
Q	106 000	390	33 000

[a] **bR** = light-adapted bacteriorhodopsin.

from those of the **P** or **P**-like states reported previously (445 vs 490 nm).[3,10] The most plausible explanation for this observation is that the thin film and acrylamide environments of the previous studies stabilize the higher wavelength species, $\mathbf{P}_{525}$.

Of particular interest in these spectra is the significant change in the intensity of the 280 nm peak associated with the aromatic residues in the protein. The experimental studies of Popp et al.,[3] and later studies on the similar pink membrane,[9] have indicated that the 13-methyl group of the 9-cis chromophore in the **P** state interacts with the aromatic residues in the binding site. This interaction is likely to be responsible for the formation of **Q** from **P** because the steric strain of 9-cis retinal in the **P** state is high enough to favor a detached chromophore. As indicated earlier, the change in the 280 nm band for the **P** state is believed to be an artifact of the deconvolution process because of the low conversion (~10%) and signal-to-noise ratio in the original data. The ~4% reduction and regeneration in this band for the **Q** state, however, is fully reproducible in those spectra with a high conversion to **Q** state (~40%). Strong steric interaction of the chromophore with the aromatic residues in the binding site would induce a significant shift in the 280 nm bands of both **P** and **Q** as the protein changes conformation to accommodate a 9-cis chromophore.

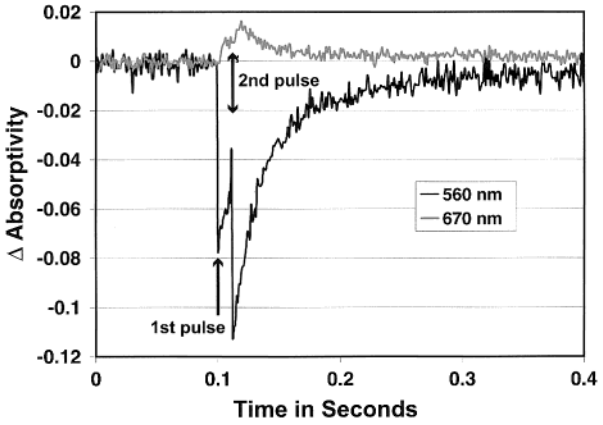

Figure 7. Time-resolved absorption at two wavelengths showing the loss of **bR** (560 nm) and the rise of the **O** state (670 nm). This plot also shows the timing of the laser pulses used in the sequentially pulsed experiment. The **O** state reaches maximum concentration roughly 10 ms following the initial laser excitation pulse at 560 nm, and the second pulse was adjusted to coincide with maximum **O** state concentration.

d. Temporal Kinetic Studies and a New P State Model. Recent studies have indicated that a path may exist directly from **bR** to **P**, in addition to the **O** → **P** photocycle branch.[10,11] A temporal approach using a tunable pulsed laser was used to determine which of these paths dominates the rate of formation of 9-cis photoproducts (Figure 2). Spectra obtained from illumination of **bR** (observed by the absorbance change at 560 nm) and **K** were compared to spectra in which the **O** state (observed by the absorbance change at 670 nm) was illuminated at the time of its maximum concentration. The same average power density was retained for both experiments.

An initial study of the photocycle of BR under these conditions (85% glycerol, pH 7, 40 °C) was performed to determine the proper timing sequence for these experiments with 568 nm pulses. From this study, the peak population of **O** was found to occur 10 ms after illumination, while the photocycle was found to be >99% complete after 1 s following either single or double (two pulses, 10 ms apart) illumination. Figure 7 illustrates that these timing parameters allow for the optimal illumination of the **O** state without a significant accumulation of other photocycle intermediates. A wavelength of 635 nm was chosen for the experiments described below, because it is red enough to produce a high-conversion photostationary state of **P**, while at the same time generating a significant proportion of fast photocycle intermediates (**K**, **L**, **M**, **N**, and **O**) from the **bR** state.

Figure 8 shows the results of two temporal kinetic experiments on an 85% (v/v) glycerol suspension of purple membrane at 40 °C. In the first case, the sample was exposed to two 635 nm, 70 mJ/cm^2 laser pulses of 3 ns duration with temporal

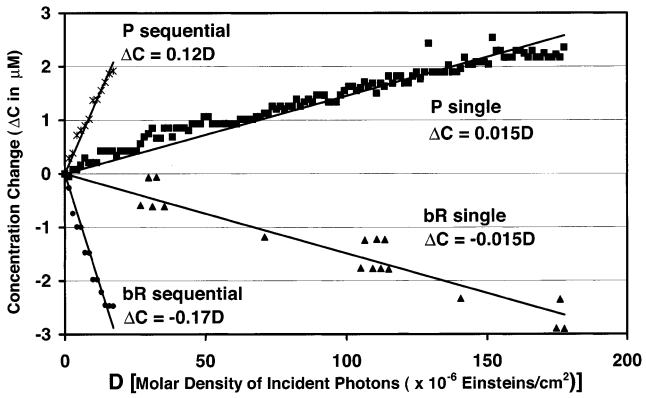

Figure 8. Photokinetic analysis of the formation of the **P** state(s) and loss of **bR** in a sample at pH 7 in 85% (v/v) glycerol during exposure to either a single pulse (single) or two sequential pulses (sequential) 10 ms apart. In both experiments, the single pulses or the first pulse of a fast sequential pair was separated by 1 s. The horizontal axis represents the cumulative number of moles of photons per unit area incident on the sample. These results provide further evidence that the primary source of the **P** state(s) is photoexcitation of the **O** state.

separation of 1 s. Our time-resolved spectral data indicated that more than 99.9% of the resting state was populated after 1 s. In the second case, two 635 nm pulses of less than half the energy density (30 mJ/cm^2) were incident on the sample with a delay of 0.99 s between each set of two pulses and a delay of 10 ms between pulse pairs. Thus, the second pulse of the pair intercepts a large accumulation of the **O** state (Figure 7). The resulting difference spectrum was deconvoluted assuming a three-species kinetic model containing the previously calculated spectra of **bR**, $\mathbf{P}_{445}$, and **Q** for these conditions. The relative amounts of $\mathbf{P}_{525}$ and the fast-decaying **K** through **O** intermediates are assumed not to make any significant contribution because of the elevated temperature (which increased all reaction rates), the long delay between exposures and spectra (~1 s), and the large number of spectra averaged (1000). To make the results of the two experiments as comparable as possible in Figure 8, the time axis was converted to the molar density of photons in einstein/cm^2, *D*. As can be seen from Figure 8, the initial yield of **P** formation, k_P (assuming a linear constant at high concentrations of BR), is more than 8 times higher when the second pulse illuminates a significant concentration of photocycle intermediates (k_P = 0.12 M/(einstein/cm^2)) than when **bR** is the sole species being irradiated (k_P = 0.015 M/(einstein/cm^2)). This result is consistent with the holographic studies performed by Popp et al.,[3] which indicated a strongly favored reaction pathway branching from a red-absorbing intermediate of the standard BR photocycle, specifically the **O** state.

One explanation for the significant amount of **P** and **Q** state formed in the single pulse experiment (Figure 8) is the existence of a small quantity of blue membrane in the sample, which when exposed to red light has been shown to form pink membrane, a species spectrally very similar to **P**.[9,23−26] A small amount of denaturation could also be occurring in this experiment as a result of the high peak power of the OPO system (~20 MW/cm^2). Such an effect has been shown to occur in purple membrane suspensions exposed to a similar peak power density (~1 MW/cm^2) at 532 nm.[27] The literature [27,28] often refers to this high peak power induced denatured form as pseudo-bR (λ_{max}= 370 nm), and it is invariably accompanied by light-induced blue membrane (**LIBM**). It is possible that photoexcitation of **LIBM** will produce a **P**-like state in the same fashion as photoexcitation of blue membrane produces the pink membrane.

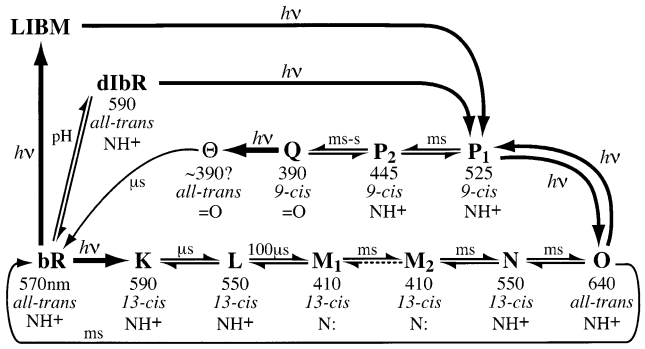

Figure 9. Possible photochemical and thermal pathways involving the **P** and **Q** states of bacteriorhodopsin. The present study provides evidence that the major source of the **P** state is a photochemical branching reaction from the **O** state, but under certain conditions, the **P** state can be formed via direct photochemical activation of species in thermal equilibrium with **bR**. The primary source is likely to be blue membrane, which is in equilibrium with **bR** at nominal and low pH. We cannot exclude direct formation of the **P** state by excitation of the laser-induced blue membrane (**LIBM**).

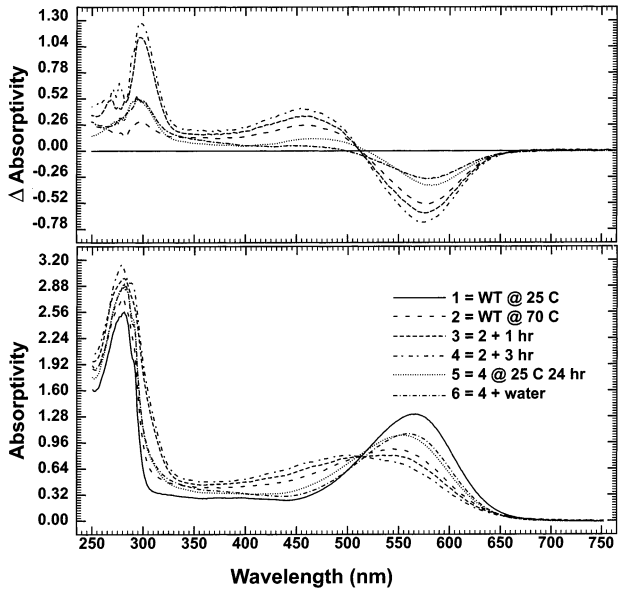

Figure 10. Spectra of **bR** in 85% glycerol heated to 70 °C for 200 min and subsequently cooled to 25 °C and rehydrated. The spectrum of the rehydrated sample was normalized to the 280 nm peak of spectrum 5. Significant differences can be seen at 300 nm after heating and at 370, 450, and 560 nm following rehydration.

Figure 9 provides spectroscopic evidence to suggest that the **P** state consists of two components, $\mathbf{P}_{525}$ and $\mathbf{P}_{445}$. Photoactivation of the **O** state generates $\mathbf{P}_{525}$ and provides the dominant pathway for the formation of **P** (and subsequently **Q**). There are two alternative paths that can also photochemically generate **P**, and these involve direct photochemical activation of either deionized BR (**dIbR**, or blue membrane) or **LIBM**. While our experiments showed no evidence of **LIBM** formation (we did not use high laser power), it is nearly impossible to eliminate the presence of small amounts of blue membrane (see discussion in ref 29).

e. Thermal Denaturation Experiments and Chromophore Analysis. Figure 10 shows several spectra of BR in 85% glycerol before, during, and after heating to 70 °C. This temperature was chosen to avoid excessive denaturation of the protein, as has been demonstrated in other studies at higher temperatures.[30,31] Purple membrane suspensions heated as high as 60 °C have been shown to contain only 13-cis and all-trans

TABLE 2: Chromophore Composition of Photochemical and Thermal Species Determined via Chromophore Extraction and HPLC

experiment (product)	% all-trans	% 13-cis[a]	% 9-cis	% 7-cis	% *A* loss at λ_{max}[b]
native (BR)	74	26	0	0	0
30 min at 647 nm[c] ($\mathbf{P}_{445}$)	65	27	8	0	11
18 h at 647 nm[c] (**Q**)	27	26	47	0	43
70 °C, 90 min	52	20	25	3	37
70 °C, 200 min, rehydrated	57	24	18	1	20

[a] The presence of 13-cis isomer is due largely, if not solely, to dark adaptation in the samples during the experiment and prior to extraction. [b] This column indicates the percent loss of chromophore absorbance at 570 nm, which is calculated by using the equation $100\% \times A/A_0$, where A_0 is the initial absorbance and A is the absorbance after exposure to light or temperature as shown in column 1. [c] Excitation at 647 nm from 50 W mercury−xenon arc lamp passed through a 647 ± 40 nm band-pass filter providing an intensity of 30 ± 3 mW/cm^2 at the sample.

chromophores.[18] In the first experiment, the sample was left to regenerate for 24 h. Unlike previous work on the first thermally generated state,[18,30] the sample did not completely recover the original spectrum following cooling. We tentatively attribute the permanent spectral change to dehydration because the microcuvette containing the sample, although sealed, provided a large open air pocket into which water could evaporate. Therefore, in the second experiment, water was added following cooling. The consequent spectrum showed a loss in the 460 nm product accompanied by an increase in the unbound (340−400 nm) and bound (500−600 nm) chromophore bands. This observation indicates that, similar to the photochemical **P** state, two states comprise the 460 nm product. The irreversible rise at 300 nm is characteristic of thermally denatured protein[30] and indicates that the thermal denaturation products are less stable than the spectrally similar **P** and **Q** states. Additionally, the kinetic behavior of the **Q**-like thermally denatured state does not resemble that of its photochemical counterpart and cannot be driven back to the **bR** resting state upon exposure to violet light (data not shown). This state shifts further to the ultraviolet (300 nm) at elevated temperatures.

Table 2 lists the results of the chromophore analysis studies. The mild thermal denaturation products of BR contain a predominately 9-cis chromophore (25% and 18%) with a very small fraction of the 7-cis isomer (3% and 1%). A 7-cis chromophore, however, does not appear in the extractions of **P** and **Q** indicating that the photochemical states differ from the similar blue states generated via thermal stress. The rehydrated thermal sample shows a marked decrease in the proportion of the 9-cis chromophore (18% vs 25%). In conjunction with the change in the UV−visible spectrum, this observation indicates that the 9-cis containing portion of the 460 nm absorbing product both denatures to a ~340 nm absorbing species and regenerates thermally to the **bR** state upon rehydration. Additionally, the dehydrated (70 °C, 90 min**)** sample shows the least agreement between the percentage of 9-cis chromophore (25%) and the percent loss in absorbance at the chromophore λ_{max} (37%). This difference all but disappears upon rehydration (18% and 20%, respectively). Such a result can be explained in terms of the additional 13-cis retinal-containing species that form when BR is heated above room temperature, causing a blue-shift in the spectrum of dark-adapted **bR**.[18] Some of the 13-cis-containing product is "trapped" in the glycerol suspension when the sample is dehydrated and cooled back to room temperature. Once the sample is rehydrated, however, this equilibrium shifts such that the spectrum of the **bR** state is recovered.

f. Comparison with Previous Studies. The work of Dancsházy and Tokaji[10,11] demonstrated that continuous broad band (λ > 500 nm) illumination of bacteriorhodopsin results in bleached photoproducts that absorb at 390 and 490 nm (after singular value decomposition). They proposed a three-state model consisting of a light sensitive state (A) in equilibrium with a primary photoproduct (B) and a presumably thermal product (C) that is photochemically irreversible and produced from the primary photoproduct (B): A ↔ B → C. "A" was assumed to be the **bR** resting state, "B" the 490 nm absorbing state, and "C" the 390 nm absorbing state. The 390 nm absorbing state was reported to be reversible to the **bR** resting state upon illumination with blue light.[11] In addition, the authors note that the photobleached state is stable and might have practical applications; however, their regeneration studies indicated a **bR** recovery rate of less than 80%, thus imposing a severe limitation on applications that require full write−read−erase capabilities.

The branched photocycle intermediates **P** and **Q** bear a strong similarity to the photobleaching products described by Dancsházy and Tokaji.[10,11] However, the nature of the experimental setup used in their study (continuous broad-band illumination) does not permit differentiation between linear and branched reaction pathways.

The results described herein support some of the models proposed in previous work,[3,10,11] while demonstrating that **P** and **Q** are stable and can be driven back to **bR** quantitatively under the appropriate conditions. Evidence for the Schiff base hydrolysis mechanism of **P** → **Q** is presented, along with data confirming that these 9-cis states are produced predominantly as a result of branching from the main BR photocycle. There appears to be a direct route to the **P** state from **bR** (or species in thermal equilibrium with **bR**), which may be due to a contribution from a small equilibrium concentration of blue membrane. Previous studies have shown that the primary photoproduct of **dIbR** is a 9-cis species analogous to **P** and denoted as the pink membrane.[9,23−25,32] The **P** state is also shown to be a mixture of two species ($\mathbf{P}_{525}$ and $\mathbf{P}_{445}$) that behave much like the two components of pink membrane ($\mathbf{dIbR}_{485}$ and $\mathbf{dIbR}_{455}$). But this comparison must be made with caution because there are some differences that remain to be explained.

In contrast to previous studies,[10,11] we demonstrate here that **bR** can be regenerated fully from the **P** and **Q** states. The reformation of the 280 nm molar absorptivity from the **Q** state is the most significant result of the regeneration experiments because it indicates that the protein, including the chromophore binding site, is not permanently modified by conversion of the protein to the **P** and **Q** states.

The thermal denaturation and chromophore extraction experiments demonstrate that the thermal products of **bR**, while having similar electronic spectra and chromophore compositions, differ significantly from **P** and **Q** in terms of chemical behavior and stability. The major differences are as follows: (1) only partial regenerability of **bR** from the **P**-like thermal species upon cooling, (2) the small, but significant, presence of the 7-cis chromophore, and (3) the formation of an irreversibly denatured, 300 nm absorbing product from the **Q**-like state upon longer exposure to elevated temperature (70 °C). Most important, these thermal products will not fully revert to **bR** upon exposure to blue light.

4. Comments and Conclusions

Bacteriorhodopsin-based optical memory devices have demonstrated potential.[4,7,33,34] The presence of a branched photocycle

reaction enables three-dimensional optical storage, whereby the **P** and **Q** states collectively represent *binary 1* and the **bR** resting state represents *binary 0*.[4] The **Q** state can also be utilized for holographic applications.[3] The ability to completely convert **P** and **Q** back to **bR** without denaturation is important for the application of BR in any practical memory device. The present study indicates that a long-lived **P** state is undesirable in a volumetric memory because the **P** state establishes an equilibrium mixture of two components with a long wavelength tail associated with the $\mathbf{P}_{525}$ component. Attempts to read or write data with the $\mathbf{P}_{525}$ state present may produce unwanted photochemistry and potential data loss. In contrast, the **Q** state is insensitive to red, yellow, and most green (>540 nm) light. Thus, the efficient formation of **Q** is important for long-term information storage. In optimizing the overall rate and magnitude of the **bR** to **Q** photoconversion in wild-type bacteriorhodopsin, one must balance the availability of water; a compromise must be reached between the competing factors of the quantum yield of the $\mathbf{O} \rightarrow \mathbf{P}_{525}$ photochemistry and temperature sensitivity (favored at lower water concentrations) and the formation rate of **Q** (favored at higher water concentrations). The experiments reported here suggest that it will be difficult to find a polymer environment that provides optimal performance of the wild-type protein in **Q**-based data storage. However, the information presented here does provide a good perspective on the mutational strategies for optimizing the protein. This work is underway.

The molecular nature of the $\mathbf{P}_{525}$ and $\mathbf{P}_{445}$ states remains to be explored. Although both states have 9-cis protonated Schiff base chromophores, little is known about the nature of the protein−chromophore interactions. It is plausible that $\mathbf{P}_{525}$ is a species characterized by a distorted 9-cis retinal protonated Schiff base chromophore with numerous unfavorable chromophore−protein interactions (e.g., Figure 12 of ref 9). These interactions destabilize the ground state and lead to a red-shifted species. Protein relaxation leads to a chromophore that is more stable and produces the blue-shifted $\mathbf{P}_{445}$ state. But the change in the protein environment responsible for the formation of the $\mathbf{P}_{445}$ state leads to unfavorable protein−protein interactions, and hence the $\mathbf{P}_{525}$ and $\mathbf{P}_{445}$ states are in dynamic equilibrium. Solvent environment, pH, and temperature all contribute to establishing the relative steady-state concentrations. While it is interesting to compare these two states with the two components of the pink membrane ($\mathbf{dIbR}_{485}$ and $\mathbf{dIbR}_{455}$) observed by Tallent et al.,[9] caution is necessary. The model proposed for $\mathbf{dIbR}_{485}$ and $\mathbf{dIbR}_{455}$ involves distortion around the 10−11 single bond and a change in the protonation state of a nearby residue.[9] We have no direct evidence or theoretical models to support a similar mechanism coupling $\mathbf{P}_{525}$ and $\mathbf{P}_{445}$. Further work on this interesting problem would be welcome.

It is interesting to consider whether the branched photocycle is a biologically advantageous process or one which has been minimized through evolution as undesirable. One can provide a straightforward explanation of why the branched photocycle might be disadvantageous. In an environment where there is no blue light present, formation of the **Q** state is terminal and results in generatation of a yellow membrane that is an ineffective proton pump. Figure 11 shows that there is ample solar flux in the 300−420 nm region of the spectrum both at the surface and 10 cm below the surface of a simulated salt marsh. Simulations of solar radiation on a single bacterium at both regions indicate that maximal **Q** state formation is about 5% (<1% at the surface) and is of minor consequence to the proton-pumping capability of the organism. But as we examine below, the simulations lead to very different conclusions when a population of organisms is included.

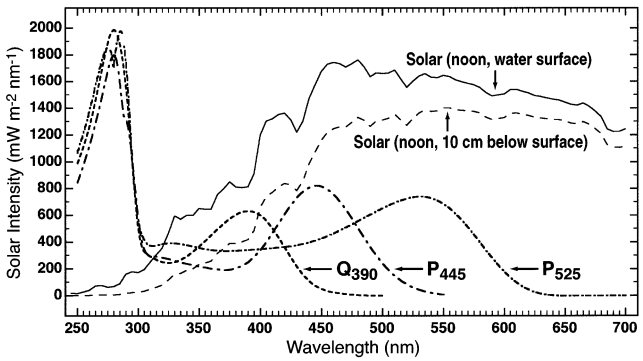

Figure 11. Comparison of the absorption spectra of the **P** and **Q** states with the terrestrial solar intensity profile at noon at the water surface[36] and 10 cm below the air−water interface of a simulated salt marsh (our data).

There may be a potential advantage to *H. salinarum* to conserve the branched photocycle. Formation of the **P** and **Q** states would provide protection by absorbing a portion of the light in the UVA (330−400 nm) and UVB (290−330 nm) regions. While UV light is damaging to most bacteria and archae, *H. salinarum* is more tolerant of UV radiation.[35] Could the branched photocycle contribute to this tolerance? When a simulation is carried out including many layers of bacteria, it is apparent that **P** and **Q** state formation provides significant UVA and partial UVB protection for those organisms 5−20 cm below the surface. At this depth, the amount of UVA and UVB radiation is limited and red light dominates, favoring accumulation of **P** and **Q** (Figure 11). Organisms at the surface, however, will be exposed to UVB because the available UVA light will rapidly photorevert the **Q** state. The fact that those organisms lying underneath layers of stacked archae could receive rather significant protection from UVA and UVB due to **P** and **Q** formation cannot be ignored. There are many examples in biology of group selection whereby a derived trait provides greater benefit to the population than to the individual.

We do not yet have the necessary quantum yield data to carry out a rigorous simulation of the potential ability of the branched photocycle to serve as a dynamic UVA or UVB screen or both. In particular, we need more accurate measurements of the quantum yields for photoreversion of **P** and **Q** back to **O** and **bR**. The fact that approximately 15% of the random mutants that we have studied diminish the efficiency of the branching reaction suggests that evolution has had ample opportunity to more fully eliminate this side reaction and has selected either to ignore branching capability or to maintain its current level. We conclude that the biological importance of the branching reaction deserves further scrutiny.

Acknowledgment. Partial support for this research was provided by the National Science Foundation (Grant EIA-0129731), the Army Research Office (MURI, Grant DAAD 19-99-1-0198), and the National Institutes of Health (Grant GM-34548). Funding for K. Jordan and S. Fyvie was provided by an NSF-REU grant (CHE-9732366). We thank Prof. N. Hampp for interesting and helpful discussions.

References and Notes

(1) Luecke, H.; Schobert, B.; Richter, H. T.; Cartailler, J. P.; Lanyi, J. K. *J. Mol. Biol.* **1999**, *291*, 899.

(2) Lanyi, J.; Pohorille, A. *Trends Biotechnol.* **2001**, *19*, 140.

(3) Popp, A.; Wolperdinger, M.; Hampp, N.; Bräuchle, C.; Oesterhelt, D. *Biophys. J.* **1993**, *65*, 1449.
(4) Birge, R. R.; Gillespie, N. B.; Izaguirre, E. W.; Kusnetzow, A.; Lawrence, A. F.; Singh, D.; Song, Q. W.; Schmidt, E.; Stuart, J. A.; Seetharaman, S.; Wise, K. J. *J. Phys. Chem. B.* **1999**, *103*, 10746.
(5) Hampp, N. *Appl. Microbiol. Biotechnol.* **2000**, *53*, 633.
(6) Hampp, N.; Thoma, R.; Zeisel, D.; Bräuchle, C. *Adv. Chem.* **1994**, *240*, 511.
(7) Millerd, J. E.; Rohrbacher, A.; Brock, N. J.; Chau, K. C.; Smith, P.; Needleman, R. *Opt. Lett.* **1999**, *24*, 1355.
(8) Tallent, J.; Song, Q. W.; Li, Z.; Stuart, J.; Birge, R. R. *Opt. Lett.* **1996**, *21*, 1339.
(9) Tallent, J. R.; Stuart, J. A.; Song, Q. W.; Schmidt, E. J.; Martin, C. H.; Birge, R. R. *Biophys. J.* **1998**, *75*, 1619.
(10) Dancsházy, Z.; Tokaji, Z.; Der, A. *FEBS Lett.* **1999**, *450*, 154.
(11) Dancsházy, Z.; Tokaji, Z. *FEBS Lett.* **2000**, *476*, 171.
(12) Ebrey, T.; Koutalos, Y. *Prog. Retinal Eye Res.* **2001**, *20*, 49.
(13) Stuart, J. A.; Birge, R. R. Characterization of the primary photochemical events in bacteriorhodopsin and rhodopsin. In *Biomembranes*; Lee, A. G., Ed.; JAI Press: London, 1996; Vol. 2A; p 33.
(14) Mathies, R.; Lin, S.; Ames, J.; Pollard, T. *Annu. Rev. Biophys. Biophys. Chem.* **1991**, *20*, 491.
(15) El-Sayed, M.; Logunov, S. *Pure Appl. Chem.* **1997**, *69*, 749.
(16) Oesterhelt, D.; Stoeckenius, W. *Methods Enzymol.* **1974**, *31*, 667.
(17) Becher, B. M.; Cassim, J. Y. *Prep. Biochem.* **1975**, *5*, 161.
(18) Scherrer, P.; Mathew, M. K.; Sperling, W.; Stoeckenius, W. *Biochemistry* **1989**, *28*, 829.
(19) Noll, G. N.; Becker, C. *J. Chromatogr., A* **2000**, *881*, 183.
(20) Maeda, A.; Iwasa, T.; Yoshizawa, T. *Biochemistry* **1980**, *19*, 3825.
(21) Fischer, U. C.; Towner, P.; Oesterheldt, D. *Photochem. Photobiol.* **1981**, *33*, 529.
(22) Maeda, A.; Tatsuo, I.; Yoshizawa, T. *Photochem. Photobiol.* **1981**, *33*, 559.
(23) Pande, C.; Callender, R. H.; Chang, C. H.; Ebrey, T. G. *Biophys. J.* **1986**, *50*, 545.
(24) Chang, C.-H.; Liu, S. Y.; Jonas, R.; Govindjee, R. *Biophys. J.* **1987**, *52*, 617.
(25) Chung-Ho, C.; Jonas, R.; Ebrey, T. G.; Hong, M.; Eisenstein, L. Protonation changes in the interconversions of the pink membrane, blue membrane and purple membrane. In *Biophysical studies of retinal proteins*; Ebrey, T. G., Frauenfelder, H., Honig, B., Nakanishi, K., Eds.; University of Illinois Press: Champaign, IL, 1987; p 156.
(26) Gross, R. B.; Todorov, A. T.; Birge, R. R. The wavelength-dependent refractive index change associated with the blue to pink membrane photochemical conversion in bacteriorhodopsin. In *Applications of Photonic Technology*; Lampropoulos, G. A., Ed.; Plenum Press: New York, 1995; p 115.
(27) Czege, J.; Reinisch, L. *Photochem. Photobiol.* **1991**, *53*, 659.
(28) Masthay, M. B.; Sammeth, D. M.; Helvenston, M. C.; Buckman, C. B.; Li, W.; Cde-Baca, M. J.; Kofron, J. T. *J. Am. Chem. Soc.* **2002**, *124*, 3418.
(29) Li, Q.; Bressler, S.; Ovrutsky, D.; Ottolenghi, M.; Friedman, N.; Sheves, M. *Biophys. J.* **2000**, *78*, 354.
(30) Cladera, J.; Galisteo, M. L.; Dunach, M.; Mateo, P. L.; Padros, E. *Biochim. Biophys. Acta* **1988**, *943*, 148.
(31) Muller, J.; Munster, C.; Salditt, T. *Biophys. J.* **2000**, *78*, 3208.
(32) Liu, S. Y.; Ebrey, T. G. *Photochem. Photobiol.* **1987**, *46*, 263.
(33) Birge, R. R.; Parsons, B.; Song, Q. W.; Tallent, J. R. Protein-based three-dimensional memories and associative processors. In *Molecular Electronics*; Ratner, M. A., Jortner, J., Eds.; Blackweel Science Ltd.: Oxford, U.K., 1997; p 439.
(34) Hampp, N.; Popp, A.; Bräuchle, C.; Oesterhelt, D. *J. Phys. Chem.* **1992**, *96*, 4679.
(35) Martin, E. L.; Reinhardt, R. L.; Baum, L. L.; Becker, M. R.; Shaffer, J. J.; Kokjohn, T. A. *Can. J. Microbiol.* **2000**, 180.
(36) Wenham, S. R.; Green, M. A.; Watt, M. E. *Applied Photovoltaics*; Bridge printery: Sydney, Australia, 1994.